

Increased flux pinning upon thermal-neutron irradiation of uranium-doped $\text{YBa}_2\text{Cu}_3\text{O}_7$

R. L. Fleischer, H. R. Hart, Jr., K. W. Lay, and F. E. Luborsky
General Electric Research and Development, Schenectady, New York 12301
 (Received 13 February 1989)

To assess fission-fragment damage as flux-pinning centers, sintered compacts of $\text{YBa}_2\text{Cu}_3\text{O}_7$ were prepared with uranium additions of 150 and 380 atomic ppm and exposed to thermal neutron fluences of 4.3×10^{17} , 1.2×10^{18} , and $4.0 \times 10^{18}/\text{cm}^2$. Magnetic hysteresis measurements were made as functions of temperature at fields up to 2.5 T. The hysteresis at 1 T for the sample containing 150 ppm uranium increased upon an irradiation of $1.2 \times 10^{18}/\text{cm}^2$ by 3.7 times at 4.5 K, 20 times at 63 K, and 8.3 times at 77 K. Much smaller increases in magnetic hysteresis were observed in undoped samples exposed to thermal neutrons. Critical-current densities were calculated from the hysteresis observed at 1 T using the critical-state model, assuming the currents to be restricted to the grains ($\approx 5 \mu\text{m}$ radius). For the 150 ppm, $1.2 \times 10^{18}/\text{cm}^2$ sample, the 1-T intragranular critical-current densities obtained are 1.5×10^7 , 1.0×10^6 , and $1.4 \times 10^5 \text{ A}/\text{cm}^2$ at temperatures of 4.5, 63, and 77 K, respectively. The critical temperatures by an ac susceptibility technique showed that the $4 \times 10^{18}/\text{cm}^2$ irradiation lowered the onset critical temperatures only slightly, from 91 to 90 K and from 91.5 to 89 K for the 150 and 380 ppm samples, respectively.

I. INTRODUCTION

The discovery of superconductors with critical temperatures above 77 K has greatly improved the prospect of widespread practical application of superconductivity.¹ Unfortunately, there are still major hurdles to be overcome before such prospects can be realized. In particular, the critical-current densities of sintered, polycrystalline high-temperature superconductors are much too low, especially in useful magnetic fields at higher temperatures.^{2,3} It appears that the intergranular superconductive coupling in polycrystalline materials is very weak and that flux pinning within grains is low, leading to very rapid flux creep and low-critical-current densities even in single grains. The present study deals with the weak intragranular flux pinning.

The pinning of flux within bulk type-II superconductors is caused by imperfections in the lattice. For traditional practical low-temperature superconductors such as Nb-Ti or Nb_3Sn , such imperfections or pinning centers include dislocations, grain boundaries, and nonsuperconducting inclusions or voids.^{4,5} For the newer, high-temperature superconductors it is not clear what the naturally occurring weak pinning centers are, though twin boundaries have been suggested for Y-Ba-Cu-O.⁶ The traditional methods of introducing lattice defects, such as cold work and grain-boundary control through heat treatment, appear not to be useful for the new materials; they are brittle and their grain boundaries are so weak that they increase the movement of flux instead of decreasing it. Another approach which has been shown effective in the older, low-temperature superconductors is the introduction of pinning centers by radiation damage. In the present study we have introduced fission-fragment damage by doping Y-Ba-Cu-O with uranium and exposing the material to thermal neutrons, inducing fission of

the uranium. We had found earlier⁷ that fission-fragment damage increased flux pinning in Nb_3Al and V_3Si .

Many forms of nuclear radiation have been used on $\text{YBa}_2\text{Cu}_3\text{O}_7$ and related oxide superconductors, with mostly consistent results. Among the radiations used are fast neutrons,⁸⁻¹⁴ protons from 0.3 to 800 MeV,¹⁵⁻¹⁷ heavy ions from 0.005 to 16 MeV/amu,¹⁸⁻²⁴ electrons at 2 MeV (Ref. 25) and 56 MeV,¹⁷ and 1.3 MeV γ rays.²⁶ The present work reports effects of fission fragments and of thermal neutrons. Most of the prior work shows consistent results in which T_c decreases, intragranular flux pinning and critical-current density (J_c) increases, and transport (intergranular) J_c decreases.

The special opportunity that is envisioned in inducing fission is that the fraction of dispersed, isolated point defects is minimized relative to clumps of displaced atoms and disordered material, which are expected to be more effective pinning centers. Thus, greater flux pinning should be created before the total damage begins to degrade the critical temperature seriously.

II. SAMPLE PREPARATION

Sintered compacts were formed from three starting compositions: $\text{YBa}_2\text{Cu}_3\text{O}_7$ plus 0, 0.08, and 0.2 weight percent of UO_2 (0, 150, and 380 atomic ppm U). Natural uranium was used. Yttrium oxide, copper oxide, uranium dioxide, and barium carbonate were ball milled in methanol with zirconia balls for 4 h. After drying for 4 h under heat lamps, the powders were screened -28 mesh. Calcining was done in air in an alumina tray at 955°C for 24 h. The powder after calcining was quite friable. It was milled for 2 h in heptane using a few drops of Grace Chemicals Hamposyl-O as a wetting agent. Drying was done under nitrogen at 50°C. X-ray diffraction analysis just prior to irradiation showed only the $\text{YBa}_2\text{Cu}_3\text{O}_7$

phase. Minor phases were, however, present as will be noted later. No identification of the microstructural location of the uranium was possible by x rays. The powders were die pressed at 12 000 psi and sintered in oxygen. The heating rate was 200 °C/h to 955 °C, where the samples were held for 8 h. Cooling was also done in oxygen. Cooling to 400 °C took 4 h, and the samples were held at 400 °C for 2 h before cooling to room temperature. The sample densities were 5.62, 5.45, and 5.66 g/cm³ for the 0, 0.08, and 0.20 wt. % samples. Bars about 3.5 × 3.5 × 5 mm³ were cut from the fired samples for irradiation and testing.

III. IRRADIATION OF SAMPLES

The samples, sealed in fused quartz tubes under $\frac{1}{2}$ atm of oxygen, were exposed to thermal neutrons (ratio of < 1 MeV to > 1 MeV, 1700:1) in Port V-11 of the Vertical Irradiation Thimble of the Brookhaven High Flux Beam Reactor. The nominal background temperature during irradiation was 60 °C; the highest temperature was less than 100 °C. The samples were exposed to nominal fluences of 2×10^{15} , 4×10^{17} , 1.2×10^{18} , and 5×10^{18} thermal neutrons/cm², values later determined to be $2.09(\pm 0.18) \times 10^{15}$, $4.29(\pm 0.13) \times 10^{17}$, $1.23(\pm 0.05) \times 10^{18}$, and $3.99(\pm 0.13) \times 10^{18}$ by fission track counting in glass dosimeters.²⁷

The resulting radioactivity decayed with the 2.7 d half-life of ⁹⁰Y, the product of neutron capture by ⁸⁹Y. Later, the decay slowed, being controlled by the spectrum of decay times of the uranium fission products.²⁸ As a result, early radioactivity is nearly equal for samples of the same size, regardless of uranium content. Later the dominant fission decay shows the expected 2.5:1 activity ratio expected for samples with 380 and 150 ppm of uranium.

Fission fragments for ²³⁵U have a double-peaked mass and energy distribution with an average of mass of 117 and energy of 84 MeV. Our maximum internal concentration of fission events of 5.1×10^{14} /cm³ was designed to approach (within a factor of 2) that known to have a large effect on the critical current of V₃Si at 1–3 T.⁷ The concentration is given by $31 \times 10^{-8} \phi c$, where ϕ is the neutron fluence in cm⁻² and c , the uranium concentration, is in atom fraction/10⁶. Given that the sum of the ranges of the two fragments from a fission event is 16 μm, the maximum internal dose may also be thought of as 4×10^{11} fission fragments/cm².

IV. MEASUREMENT OF FLUX PINNING BY MAGNETIC HYSTERESIS

The measurements of the change in bulk flux pinning upon fission-fragment irradiation are the primary results of this study. Two potential measures of flux pinning are magnetic hysteresis and transport critical current. For polycrystalline samples the transport critical-current density is strongly dependent on the usually very poor intergrain coupling. Since the intergrain coupling was expected to remain poor or even to degrade under irradiation,^{11,19–21} magnetic hysteresis was chosen for this study. The primary results are present as magnetic hys-

teresis (emu/cm³) at a field of 1 T measured as a function of temperature (4–77 K). In a later section the magnetic hysteresis will be discussed as the intragranular critical-current density computed from the critical-state model.

In order to measure the magnetic hysteresis loops, a Princeton Applied Research vibrating-sample magnetometer was used with a 3 T electromagnet. The current in the electromagnet was programmed with a triangular wave form in order to generate the *M-H* curve; saturation of the iron in the electromagnet resulted in a nonlinear field sweep. The field was measured by a Hall probe placed in the gap of the magnet. An ac signal proportional to the magnetization was detected by pick-up coils arranged to cancel out common-mode noise. The output of the coils was amplified by a lock-in amplifier using a 100-ms filter time constant. The outputs of the Hall probe (field) and lock-in (magnetization) were fed to an x-y recorder. Calibration of the magnetization scale was done by measuring the saturation flux from a disk of pure nickel of known weight. The sample was mounted with the long axis perpendicular to the magnetic field. Demagnetization effects are negligible (< 1.5%) for the magnetizations observed at 1 T.

A Janis helium cryostat, a Lake Shore temperature controller, and a carbon-glass resistance thermometer were used to control the temperature in the range 4–77 K. At each temperature, after the temperature was stabilized, the sample was run through one ±2.5 T field cycle before recording the *M-H* curve. A constant sweep rate of current corresponding to a 1000 s period was used.

M-H curves at 35 K for irradiated (4×10^{18} /cm²) and unirradiated samples (150 atomic ppm U) are shown in Fig. 1. The arrows at 1 T indicate the definition of hysteresis ΔM used in the following discussions: ΔM is the full difference in magnetization. The data are the average of the ΔM 's obtained at +1 T and at -1 T. In order to determine the sensitivity of the hysteresis to the rate of field sweep, ΔM at 1 T was measured for field sweep periods ranging from 20 to 2000 s for the samples and

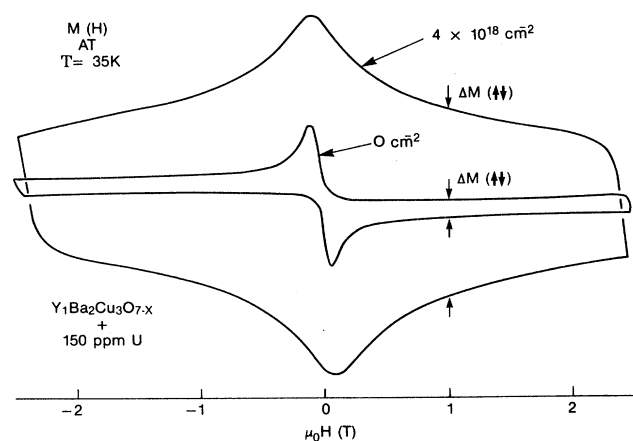


FIG. 1. Tracings of the magnetization vs magnetic field for two uranium-doped (150 atomic ppm) samples of Y-Ba-Cu-O exposed to 0 and 4×10^{18} thermal neutrons/per cm², respectively. The field was cycled with a period of 1000 s. The magnetic hysteresis at 1 T is indicated by ΔM and the associated arrows.

temperature shown in Fig. 1. The hysteresis at ± 1 T was found to decrease linearly with the logarithm of the period, with a total change of 19% for the unirradiated sample and 12% for the irradiated sample over this 100x range in sweep period.

In Fig. 2 are the results of hysteresis measurements displayed for samples containing 150 atomic ppm of uranium in both the unirradiated and irradiated ($1.23 \times 10^{18}/\text{cm}^2$) states and an irradiated sample with no added uranium. Strong, temperature-dependent enhancement is observed. The enhancements in flux pinning are 3.7 times at 4.5 K, 20 times at 63 K, and 8.3 times at 77 K. Note that flux pinning is decreasing rapidly at liquid-nitrogen temperature.

The temperature dependence of the hysteresis indicates that the pinning energy of the fission-fragment-induced pinning centers is larger than that of the pinning centers in the unirradiated samples. In a linear plot of ΔM versus T , the $\Delta M = 0$ intercept obtained by extrapolating the low-temperature portion of the curve yields a characteristic temperature which in one model of flux pinning and flux creep is proportional to the pinning energy of the pinning centers.²² The characteristic temperatures obtained are about 12 K (unirradiated) and 30 K (irradiated).

Data for the other irradiations are presented in Table I for 4.5, 63, and 77 K. The hysteresis for the undoped samples is unchanged by a thermal neutron fluence of $4.3 \times 10^{17}/\text{cm}^2$ and increases by 10–60% for $1.2 \times 10^{18}/\text{cm}^2$. These increases are 3.7, 3.1, and 4.2% of those produced in the 150 ppm-uranium sample. Unfortunately no undoped control was irradiated at $4 \times 10^{18}/\text{cm}^2$. The hysteresis values for the 150 and 380 ppm samples are enhanced relative to both the undoped samples and the unirradiated doped samples, with a saturation of the enhancement occurring between 1.2×10^{18} and $4 \times 10^{18}/\text{cm}^2$.

Surprisingly the enhancement is essentially the same for the two concentrations of uranium, actually larger for the 150 ppm sample at the intermediate fluence of $1.2 \times 10^{18}/\text{cm}^2$. Possible explanations will be discussed in a later section. The relative values of the uranium concentrations are not at fault since the levels of radioactivi-

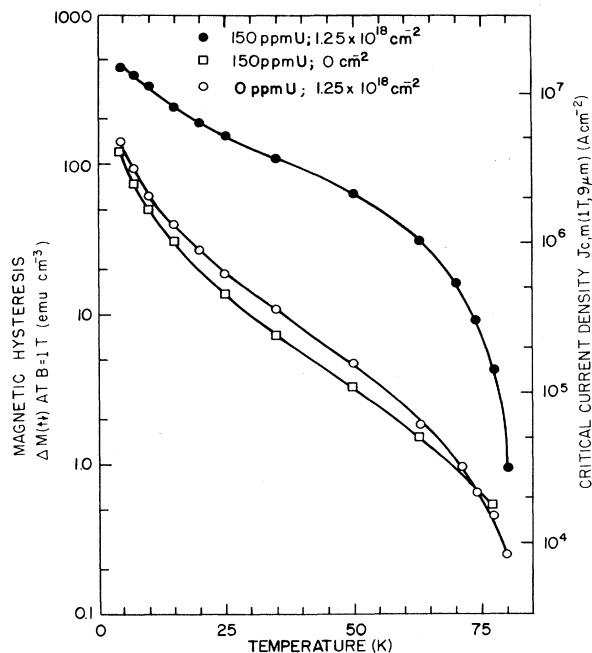


FIG. 2. Magnetic hysteresis at 1 T (left-hand scale) vs temperature for unirradiated and irradiated samples of Y-Ba-Cu-O (150 atomic ppm U) and a 0 ppm U, irradiated sample. The right-hand scale shows the intragranular critical-current density derived from magnetic hysteresis and grain size using the critical-state model.

ty in the samples (after a sufficient delay) reflects the two uranium contents. The ratio of the levels of radioactivity per unit volume is 2.2 and the ratio of the starting compositions is 2.5. The decrease in the transition temperature of the irradiated samples (see below) also reflects the higher radiation damage in the sample of higher nominal uranium content.

V. CRITICAL TEMPERATURES

Measurements of critical temperature were made for the unirradiated and irradiated ($4 \times 10^{18}/\text{cm}^2$) samples

TABLE I. Magnetic hysteresis at 1 T (emu/cm²).

U Concentration and T	Thermal neutron fluence			
	0	$4.3 \times 10^{17}/\text{cm}^2$	$1.23 \times 10^{18}/\text{cm}^2$	$4.0 \times 10^{18}/\text{cm}^2$
0 ppm				
4.5 K	128	120	141	
63 K	1.15	1.16	1.85	
77 K	0.39	0.35	0.46	
150 ppm				
4.5 K	122	143	450	303
63 K	1.50	6.31	30.5	20.7
77 K	0.52	0.90	4.32	2.56
380 ppm				
4.5 K	132	136	260	339
63 K	1.54	6.36	14.9	18.6
77 K	0.60	1.16	1.77	2.02

using a frequency-shift ac susceptibility technique.²⁹ The results are shown in Fig. 3. The irradiation lowered the onset temperatures only slightly, from 91 to 90 K and from 91.5 to 89 K for the 150 and 380 atomic ppm samples, respectively. However, the 5–95% widths were increased upon irradiation from 4 to 7 K, and 12 K for the 150 and 380 ppm samples, respectively.

VI. MICROSCOPIC CONSIDERATIONS

Transmission electron microscopy on a 380 ppm sample exposed to $2.5 \times 10^{15}/\text{cm}^2$ showed planar faults and localized regions of high dislocation density which are not commonly observed in our undoped sintered compacts. No evidence of fission-fragment tracks was seen.

Examination by transmission electron microscopy (TEM) and electron microprobe analysis (EMA) showed that the uranium was inhomogeneously distributed, with some locally concentrated in phases other than $\text{YBa}_2\text{Cu}_3\text{O}_7$, for example, in inclusions of Ba-Cu-U-O or Ba-Y-U-O. There was no indication that the uranium was located preferentially on grain boundaries. The distribution of the most abundant uranium-bearing inclusions was on a fine enough scale that all of the sample could be reached by fission fragments, given the $8 \mu\text{m}$ average range of fission fragments expected for Y-Ba-Cu-O.

Light microscopy and image analysis were used to determine the size and shape distributions of the grains of the sintered compacts for the 150 and 380 ppm samples. The average ratios of the maximum diameter to the minimum diameter were found to be 1.8 and 1.9 for the 150 and 380 ppm samples, respectively. The volume-weighted average equivalent diameters were 11.7 and $13.9 \mu\text{m}$, respectively. Finally, the volume fractions of pores were found to be 12% and 6%, respectively. In

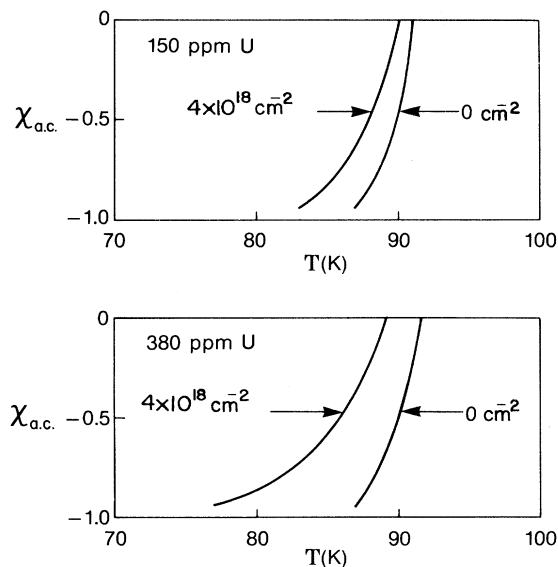


FIG. 3. Normalized ac magnetic susceptibility vs temperature for uranium-doped (atomic ppm) samples of Y-Ba-Cu-O, two of which had been irradiated with thermal neutrons to a fluence of $4 \times 10^{18}/\text{cm}^2$.

addition, the image analysis was used to determine the effective size and shape of the grains for use in calculating the intragranular critical-current density from the magnetic hysteresis by means of the critical-state model, as described in the next section.

VII. INTERPRETATION OF MAGNETIC HYSTERESIS: INTRAGRANULAR CRITICAL-CURRENT DENSITIES

The critical-state model,³⁰ together with an appropriate measurement of magnetic hysteresis, allows one to determine, for a homogeneous material, the product of the critical-current density and the dimension of the sample, $J_c D$. Unfortunately, for an inhomogeneous material such as a sintered compact the application of the critical-state model is not straightforward. At one extreme the current may flow as if the sample were homogeneous, yielding $J_{c,s} D_s$, where D_s is the dimension of the sample. At the other extreme, the grains (or even smaller entities) may be essentially isolated as far as supercurrents are concerned; in this case the product obtained is $J_{c,g} D_g$, where D_g is the dimension of the grain. Intermediate situations can occur, in which a portion of the super current flows throughout the sample and another portion is restricted to the grains. The critical-state model does not allow one to determine separately the applicable sizes of the regions and the appropriate J_c 's. There is thus an essential ambiguity in the interpretation of magnetic hysteresis by means of the critical-state model.

It is possible, in principle, to determine the applicable D and thus J_c by a destructive experiment in which the sample is ground to powder and the magnetic hysteresis is followed as the size of the powder is decreased. The magnetic hysteresis remains unchanged as long as the dimension of the sample or powder is greater than the effective D ; it decreases with size as the powder is ground into sizes smaller than D . Such experiments^{31,32} have shown that for polycrystalline sintered compacts the effective size is not the sample size, but is closer to the (much smaller) grain size. This result is to be expected if the intergrain superconductive coupling is very weak. In the present analysis the assumption is made that, at 1 T, the currents are restricted to the grains; the measured, appropriately averaged grain size is used for D and the current densities thus calculated are described as intragranular critical-current densities.

The critical-state model yields particularly simple expressions for the hysteresis for crystals of simple cross section when certain conditions are met: The applied field is large compared with H_{c1} ; the field variation across the sample is small enough that J_c varies little across the sample; and the field has been swept through a sufficiently large excursion that critical currents have been induced in the same sense throughout the sample. These conditions are met at 1 T in the present experiment. Such results are given below for two cross sections:

Circular, diameter D : $\Delta M = J_c D / 30$,

Rectangular, $S_2 > S_1$: $\Delta M = J_c (S_1 / 20) [1 - (S_1 / 3S_2)]$.

Examination of many grains in light micrographs led

to the choice of a slightly more complex cross section, a split circle joined by a rectangular midsection, for the analysis of the magnetic hysteresis. The image analysis of the grains in the light micrograph yielded D_{\max} and the

$$\Delta M = J_c \times (D_1/20) \times [1 - (1 - \pi/6)D_1/D_{\max}] / [1 - (1 - \pi/4)D_1/D_{\max}].$$

The contribution of each grain to the magnetic hysteresis was calculated and summed for several hundred grains to give the factor relating the magnetic hysteresis to the critical-current density. Such analyses were performed for the 150 and 380 ppm samples, but not for the undoped sample. For convenience of discussion and presentation the factor obtained can be related to an effective diameter using the expression given above for a circular cross section. The effective diameters are 9.0 and 10.5 μm , respectively. It should be noted that these effective diameters differ from the volume-weighted values given above; the weighting differs for the magnetic analysis.

The intragranular critical-current densities calculated are shown in Fig. 2 on the right-hand scale. The discussion of Sec. IV applies to the critical-current densities as well since the magnetic hysteresis and critical-current densities are related by a constant factor for each sample. Caution must be exercised in considering these current densities, for the use of the dimensions of the grains in the critical-state model is, as mentioned above, an oversimplification of a complex situation. If the dimensions of the sample had been used instead of the grain size, the critical-current densities calculated would have been smaller by a factor of 400. The important point is that, whether measured by magnetic hysteresis or by a derived critical-current density, fission-fragment irradiation of Y-Ba-Cu-O leads to a significant enhancement of flux pinning.

VIII. DISCUSSION

We noted earlier that one special merit of fission events is a greater localization of damage into clumps of disorder—as opposed to dispersed point defects, such as are produced, for example, by electron or γ -ray irradiation. A possibility that was considered is that track formation might occur, since fission tracks have been seen in other perovskite structures.³³ Because TEM examination found no tracks, the damage present is not from ionization, but from the 5% of the fission energy³⁴ that goes directly in to atomic collisions. Tracks were, in fact, expected not to occur, since for resistivities below about 2000 Ω cm tracks are not found.³⁵

Even so, the expected damage is more localized than that from other forms of radiation damage. Table II indicates the relative damage effectiveness of fission fragments under the assumption that each 50 eV expended in atomic collisions can, on the average, displace an atom. In addition, the fission damage is localized to within < 10 μm of the fissionable atom, whereas the mean free path for a 1 MeV neutron in $\text{YBa}_2\text{Cu}_3\text{O}_7$ is 3.1 cm and its energy will be lost through a series of collisions, not in a

single event. These parameters were used to determine for each grain its maximum and equivalent minimum dimensions, D_{\max} and D_1 . For this cross section and critical-state model yields,

single event.

The effects seen here are clearly caused by fission and not primarily by the neutron irradiation. Effects were present at thermal neutron doses as low as $4 \times 10^{17}/\text{cm}^2$ which included a fast component of only $2.4 \times 10^{14}/\text{cm}^2$. Since fast neutron doses of $\sim 5 \times 10^{16}/\text{cm}^2$ are required before appreciable effects on J_c are seen,^{12,14} the effect of the fast flux is negligible in our experiments. Thermal neutrons, via capture and γ -ray emission can produce displacements.³⁶ In this case the number is uncertain, but not necessarily small, relative to fission damage, but it is more uniformly dispersed. Using Walker's first-order formula and existing data³⁷ we calculate that less than 5.3% of the displacements could be from thermal neutrons. The accuracy of this calculation is compatible with values of 3.1%–4.2% quoted earlier. If ^{235}U were used in place of natural uranium, fission would be enhanced relative to thermal-neutron effects by 139 times.

The systematics in Table I appear to differ for the 150 ppm and the 380 ppm uranium samples. If the only distinction between the two samples were the uranium concentration, then the fission effects should be a function only of ϕc . There is a clear discrepancy since the values for 150 ppm U at $1.23 \times 10^{18}/\text{cm}^2$ ($\phi c = 1.8 \times 10^{14}/\text{cm}^2$) are greater than those for 380 ppm at $0.43 \times 10^{18}/\text{cm}^2$ ($\phi c = 1.6 \times 10^{14}/\text{cm}^2$) by factors of 3.1, 4.3, and 2.6, respectively, for 4.5, 63, and 77 K, i.e., far beyond the experimental noise. The 150 ppm data show a maximum near $1.23 \times 10^{18}/\text{cm}^2$. The 380 ppm data increase throughout the irradiation.

We recognize two possible factors that may contribute toward explaining the discrepancy. One is that the uranium distribution is different in the two samples. If, for example, 150 ppm were the solubility limit for uranium and the remaining uranium were present in other phases physically separated from the $\text{YBa}_2\text{Cu}_3\text{O}_7$, the excess uranium would affect the $\text{YBa}_2\text{Cu}_3\text{O}_7$ only to a limited extent. The data would then be expected to a first approximation to follow ϕ only, instead of ϕc , since c in the

TABLE II. Estimated displacements per particle.

Particle	Approximate number of atomic displacements
1 MeV electron	1
0.0025 eV neutron	10
1 MeV neutron	2,000
1 pair fission fragments (170 MeV)	200 000

TABLE III. Comparison with other types of irradiations (maximum magnetic hysteresis in emu/cc at 1 T).

Temperature (K)	Irradiation		
	Fast neutrons	Fast protons	Fission fragments
4.2	260 (Ref. 12)		450
7	220 (Ref. 14)	155 (Ref. 16)	400
42	52 (Ref. 12)		88
77	6.5 (Ref. 12)		4.3

superconducting phase would be constant. From scanning electron microscopy (SEM) examination we do know that some of the uranium is present in small particles, but the sensitivity of the method is not sufficient to quantify the partition of uranium between the different phases. We plan to attempt to produce samples of larger grain size so that fission-track-based uranium mapping³⁸ can resolve the distribution.

A second possibility is that at higher doses the dispersed effects of the thermal-neutron fluence becomes major and, in fact, causes the drop in magnetic hysteresis at the highest dose. A test of this possibility is more laborious. Substitution of either ²³⁹Pu or enriched uranium for natural uranium would allow the same dose of fissions at a lower dose of thermal neutrons. From Table I we know that the neutron exposure up to $10^{18}/\text{cm}^2$ enhances magnetic hysteresis. It may be that it degrades the superconductivity at higher doses. Full explanation of the effects of neutron dose and uranium concentration will require further study.

Semiquantitative comparisons can be made between the radiation-induced magnetic hysteresis or flux pinning of the present study and those of Gost *et al.*¹⁴ and Wisniewski *et al.*¹² for fast neutrons and Willis *et al.*¹⁶ for 800 MeV protons. Such comparisons are inexact because of differences in grain size in the different sintered compacts. Choosing the maximum ΔM (emu/cm³) at 1 T for each study, we have the data given in Table III. Given the uncertainties in the comparisons, the data are remarkably similar; it might be concluded that these are not radical differences in the effects of the different forms of irradiation.

It is appropriate to note that the fission dose that produced the optimum effect on magnetic hysteresis in this study is about 15% of that which was most effective⁷ for the A15 structure V₃Si. Thus these results raise the question as to whether oxide superconductors generally are more sensitive to radiation than the intermetallic compounds.

IX. CONCLUSIONS

Two previously untested types of radiation exposure of YBa₂Cu₃O₇ have been tested. Internal irradiation with fission fragments from ²³⁵U enhances the magnetic hysteresis and thus the pinning of flux. Enhancements at 1 T, ranging from 4 to 20 times, depending on temperature, are observed for a dose of 5.7×10^{13} fissions/cm³. An intragranular critical-current density of 1.4×10^5 A/cm² at 77 K and 1 T is inferred for this dose using the critical-state model. Lesser effects of thermal neutrons are seen. For 1.2×10^{18} thermal neutrons/cm² enhancements in magnetic hysteresis at different temperatures were about 4% of the effects that were produced by fission fragments.

ACKNOWLEDGMENTS

We wish to thank J. Grande, E. L. Hall, L. A. Peluso, and D. C. Rorer for their valuable assistance in this work. H. R. H. wishes to thank the School of Applied and Engineering Physics of Cornell University for its hospitality during a portion of this project.

¹M. K. Wu, J. R. Ashburn, C. J. Torng, P. H. Hor, R. L. Meng, L. Gao, Z. J. Huang, Y. Q. Wang, and C. W. Chu, *Phys. Rev. Lett.* **58**, 908 (1987).

²J. W. Ekin, A. I. Braginski, A. J. Panson, M. A. Janocko, D. W. Capone II, N. J. Zaluzec, B. Flandermeyer, O. F. de Lima, M. Hong, J. Kwo, and S. H. Liou, *J. Appl. Phys.* **62**, 4821 (1987).

³C. V. N. Rao, S. K. Agarwal, B. Jayaram, S. Takacs, and A. V. Narlikar, *Z. Metall.* **79**, 271 (1988).

⁴A. M. Campbell and J. E. Evetts, *Adv. Phys.* **21**, 199 (1972).

⁵J. D. Livingston and H. W. Schadler, *Prog. Mat. Sci.* **12**, 185 (1964).

⁶P. H. Kes, *Physica C* **153-155**, 1121 (1988).

⁷C. P. Bean, R. L. Fleischer, P. S. Swartz, and H. R. Hart, Jr., *J. Appl. Phys.* **37**, 2218 (1966).

⁸S. T. Sekula, D. K. Christen, H. R. Kerchner, J. R. Thompson, L. A. Boatner, and B. C. Sales, *Jpn. J. Appl. Phys.* **26**, Suppl. **26-3**, 1185 (1987).

⁹J. O. Willis, J. R. Cost, R. D. Brown, J. D. Thompson, and D. E. Peterson, in *High Temperature Superconductors*, Proceedings of the Materials Research Society Symposium, edited by M. B. Brodsky, R. C. Dynes, K. Kitazawa, and H. L. Tuller (Materials Research Society, Pittsburgh, 1988), Vol. 99, p. 391.

¹⁰P. Muller, H. Gerstenberg, M. Fischer, W. Schindler, J. Strobel, G. Saemann-Ischenko, and H. Kammermeier, *Solid*

- State Commun. **65**, 223 (1988).
- ¹¹H. Kupfer, I. Apfelstedt, W. Schauer, R. Flukiger, R. Meier-Hirmer, H. Wuhl, and H. Scheurer, *Z. Phys. B* **69**, 167 (1987).
- ¹²A. Wisniewski, M. Baran, P. Przysiupski, H. Szymczak, A. Pajaczkowska, B. Pytel, and K. Pytel, *Solid State Commun.* **65**, 577 (1988).
- ¹³A. Umezawa, G. W. Crabtree, J. Z. Liu, H. W. Weber, W. K. Kwok, L. H. Nunez, T. J. Moran, C. H. Sowers, and H. Claus, *Phys. Rev. B* **36**, 7151 (1987).
- ¹⁴J. R. Cost, J. O. Willis, J. D. Thompson, and D. E. Peterson, *Phys. Rev. B* **37**, 1563 (1988).
- ¹⁵G. C. Xiong, H. C. Li, G. Linker, and O. Meyer, *Phys. Rev. B* **38**, 240 (1988).
- ¹⁶J. O. Willis, D. W. Cooke, R. D. Brown, J. R. Cost, J. F. Smith, J. L. Smith, R. M. Aikin, and M. Maez, *Appl. Phys. Lett.* **53**, 417 (1988).
- ¹⁷W. G. Maisch, G. P. Summers, A. B. Campbell, C. J. Dale, J. C. Ritter, A. R. Knudson, W. T. Elam, H. Herman, J. P. Kirkland, R. A. Neiser, and M. S. Osofsky, *IEEE Trans. Nucl. Sci. NS-34*, 1782 (1987).
- ¹⁸J. C. McCallum, C. W. White, and L. A. Boatner, *Mater. Lett.* **6**, 374 (1988).
- ¹⁹G. J. Clark, F. K. LeGoues, A. D. Marwick, R. B. Laibowitz, and R. Koch, *Appl. Phys. Lett.* **51**, 1462 (1987).
- ²⁰A. E. White, K. T. Short, D. C. Jacobson, J. M. Poate, R. C. Dynes, P. M. Mankiewich, W. J. Skocpol, R. E. Howard, M. Anzlowar, K. W. Baldwin, A. F. J. Levi, J. R. Kwo, T. Hsieh, and M. Hong, *Phys. Rev. B* **37**, 3755 (1988).
- ²¹A. E. White, K. T. Short, R. C. Dynes, A. F. J. Levi, M. Anzlowar, K. W. Baldwin, P. A. Polakos, T. A. Fulton, and L. N. Dunkleberger, *Appl. Phys. Lett.* **53**, 1010 (1988).
- ²²Y. Yeshurun and A. P. Malozemoff, *Phys. Rev. Lett.* **60**, 2202 (1988).
- ²³S. V. Antonenko, I. Yu. Bezotosnyi, A. I. Grigor'ev, N. N. Degtyarenko, V. V. Evstigneev, V. F. Elesin, V. E. Zhuchkov, I. V. Zakharchenko, A. S. Molchanov, S. V. Shavkin, A. I. Golovashkin, S. I. Krasnosvobodtsev, and E. V. Pechen, *Pis'ma Zh. Eksp. Teor. Fiz.* **46**, 362 (1987) [*Sov. Phys.—JETP Lett.* **46**, 456 (1987)].
- ²⁴D. B. Chrisey, G. P. Summers, W. G. Maisch, E. A. Burke, W. T. Elam, H. Herman, J. P. Kirkland, and R. A. Neiser, *Appl. Phys. Lett.* **53**, 1001 (1988).
- ²⁵N. Moser, A. Hofmann, P. Schule, R. Henes, and H. Kronmuller, *Z. Phys. B* **71**, 37 (1988).
- ²⁶B. B. Boiko, F. P. Korshunov, G. V. Gatafskii, A. I. Akimov, V. I. Gatafskaya, S. E. Demyanov, and E. K. Strikuk, *Phys. Status Solidi A* **107**, K139 (1988).
- ²⁷R. L. Fleischer, P. B. Price, and R. M. Walker, *Nucl. Sci. Eng.* **22**, 153 (1965).
- ²⁸M. Eisenbud, *Environmental Radioactivity*, 3rd ed. (Academic, New York, 1987), p. 206.
- ²⁹A. L. Schawlow and G. E. Devlin, *Phys. Rev.* **113**, 120 (1959).
- ³⁰C. P. Bean, *Phys. Rev. Lett.* **8**, 250 (1962); *Rev. Mod. Phys.* **36**, 31 (1964).
- ³¹M. Suenaga, A. Ghosh, T. Asano, R. L. Sabatini, and A. R. Moodenbaugh, in *High Temperature Superconductors*, Proceedings of the Materials Research Society Symposium, edited by M. B. Brodsky, R. C. Dynes, K. Kitazawa, and H. L. Tuller (Materials Research Society, Pittsburgh, 1988), Vol. 99, p. 247.
- ³²K. Itoh, H. Wada, T. Kuroda, Y. Kaieda, O. Odawara, and T. Oie, *Cryogenics* **28**, 575 (1988).
- ³³C. J. Ball, R. G. Blake, D. J. Cassidy, and J. L. Woolfrey, *J. Nucl. Mater.* **151**, 151 (1988).
- ³⁴Hj. Matzke, *Radiat. Eff.* **64**, 3 (1982).
- ³⁵R. L. Fleischer, P. B. Price, and R. M. Walker, *J. Appl. Phys.* **36**, 3645 (1965).
- ³⁶R. M. Walker, *J. Nucl. Mater.* **2**, 147 (1960).
- ³⁷E. Troubetzkoy and H. Goldstein, *Nucleonics* **18**, 171 (1960).
- ³⁸R. L. Fleischer, P. B. Price, and R. M. Walker, *Nuclear Tracks in Solids* (University of California Press, Berkeley, 1975).